Supporting Information

Ba$_4$Ca(B$_2$O$_5$)$_2$F$_2$: π-Conjugation of B$_2$O$_5$ in the Planar Pentagonal Layer Achieving Large Second Harmonic Generation of *Pyro*-borate

Shuaishuai Li, [‡][a] Xiaomeng Liu, [‡][b] Hongping Wu,[a] Zhongfu Song,[a] Hongwei Yu,[*][a] Zheshuai Lin,[*][b] Zhanggui Hu,[a] Jiyang Wang,[a] and Yicheng Wu[a]

[a]*Tianjin Key Laboratory of Functional Crystal Materials, Institute of Functional Crystal, Tianjin University of Technology, Tianjin 300384, China.*

[b]*Beijing Center for Crystal R&D, Key Lab of Functional Crystals and Laser Technology of Chinese Academy of Sciences, Technical Institute of Physics and Chemistry, Chinese Academy of Sciences, Beijing 100190, P. R. China.*

CONTENTS

Experimental Details.

Reagents.

Na_2CO_3, CaO (Tianjin Fuchen Chemical Co., Ltd, 99.0%), NH_4F (Aladdin Reagent Co., Ltd, 99.99%)，$Ba(OH)_2 \cdot 8H_2O$, $BaCO_3$, BaF_2, H_3BO_3, and PbF_2 (Aladdin Chemistry Co., Ltd., 99.5%) were used as received without any further treatment.

Syntheses

The single crystals of $Ba_4Ca(B_2O_5)_2F_2$ were obtained via high-temperature solution method with a mixture of Na_2CO_3 (0.021 g), $BaCO_3$ (0.303 g), BaF_2 (0.173 g), CaO (0.038 g), H_3BO_3 (0.295 g), and PbF_2 (0.167 g) in the stoichiometric ratio of 0.6:4.5:2.9:2:14:2. The mixture was put into a platinum crucible, which was put in a vertical programmable temperature furnace. To obtain a homogeneous melt, the samples were heated to 900 °C and held for 12 hours, then cooled to 850 °C rapidly, after which they were cooled to 450 °C at a rate of 5 °C/h, subsequently cooled to room temperature by switching off the furnace. During the process of spontaneous crystallization, small single crystals were formed in the platinum crucible. Several colorless crystals could be obtained from the reaction products for further characterization by single-crystal X-ray diffraction measurements.

The polycrystalline samples of $Ba_4Ca(B_2O_5)_2F_2$ were synthesized by the conventional solid-state reaction method. $BaCO_3$ (0.614g, 3mmol), BaF_2 (0.200g, 1.1mmol), $CaCO_3$ (0.103g, 1mmol), and H_3BO_3 (0.282g, 4.4mmol), were mixed in a ceramic crucible thoroughly and preheated at 600 °C for 12 h to decompose CO_2 and H_2O. Then the mixture was calcined at 780°C for 15 h with several intermediate grindings. The phase purity of $Ba_4Ca(B_2O_5)_2F_2$ was confirmed by powder X-ray diffraction (PXRD) analysis.

Powder X-ray Diffraction (PXRD).

The phase purity of $Ba_4Ca(B_2O_5)_2F_2$ was checked out with a SmartLab9KW X-ray diffractometer (XRD) equipped with Cu-Ka radiation (λ = 1.5418 Å) at room temperature. The measured 2θ range was $10°-70°$ with a scan step size of 0.01° and a step time of 2 s.

Single-Crystal Structure Determination.

The crystal data of $Ba_4Ca(B_2O_5)_2F_2$ was collected on a Bruker SMART APEX II 4K CCD diffractometer with Mo Kα radiation (λ = 0.71073 Å) at 293(2) K, and integrated with the SAINT program[1]. The crystal structure was solved by the direct method and refined by the SHELXTL system[2]. The atomic positions of the structure were refined with anisotropic displacement parameters and secondary extinction correction.

PLATON[3] was used to check the structure for missing symmetry elements, and no higher symmetry was found.

UV-vis-NIR diffuse reflectance spectroscopy

The UV-vis-NIR diffuse reflectance data was collected using a Shimadzu SolidSpec-3700DUV spectrophotometer in the range 190 – 2500 nm. The Teflon was used as a reference. The absorption (K/S) data is calculated from Kubelka-Munk function $F(R) = (1−R)^2/2R = K/S$, where R represents the reflectance, K the absorption, and S the scattering.[4,5]

Second-harmonic generation Measurement.

Powder SHG measurements were performed by the Kurtz−Perry method [6] with 1064 nm Nd:YAG solid-state laser. Polycrystalline powder of $Ba_4Ca(B_2O_5)_2F_2$ was ground and sieved into several particle size ranges: 25−53, 53−75, 75−106, 106−120, 120−150, 150−180, and 180-212 μm, to investigate its phase-matching behavior. Polycrystalline KH_2PO_4 (KDP) was also sieved into similar particle sizes as the standard.

Infrared Spectroscopy

A Nicolet iS50 FT-IR spectrometer was used to record the IR spectrum of $Ba_4Ca(B_2O_5)_2F_2$ in the range of 400-4000 cm^{-1}. A sample of ∼10 mg was used for testing.

Thermal Analysis.

Differential scanning calorimetry (DSC) and thermogravimetric (TG) analysis were carried out on a NETZSCH STA 449C thermal analysis instrument. With the help of flowing nitrogen atmosphere condition, powder sample (~9 mg) was heated from 25 to 1000 °C at a rate of 5 °C/min

Computational Methods

The first-principles calculations for $Ba_4Ca(B_2O_5)_2F_2$ and α-$Li_4B_2O_5$ crystals are performed by the plane-wave pseudopotential[7] method implemented in the CASTEP package[8] based on the density functional theory (DFT)[9]. The exchange-correlation functional was chosen as the Perdew-Burke-Emzerhof (PBE) functional within the generalized gradient approximation (GGA)[10]. The plane-wave energy cutoff was set as 900 eV and self-consistent-field tolerance was set as $1 × 10−6$ eV/atom. The Monkhorst-Pack k-point meshes with a density of (3×3×3) and (2×5×1) points in the Brillouin zone were chosen for $Ba_4Ca(B_2O_5)_2F_2$ and α-$Li_4B_2O_5$, respectively.[11] Based on the experimentally obtained crystal structures, the electronic band structure of $Ba_4Ca(B_2O_5)_2F_2$ and α-$Li_4B_2O_5$ were calculated. And their nonlinear optical properties were calculated by the scissors-corrected PBE method.[12] Then, the second-order susceptibility $\chi^{(2)}$ and the SHG coefficient d_{ij} were calculated using an expression originally proposed by Rashkeev et al.[13] and developed by Lin et al.[14]

Furthermore, in order to more intuitively identify the orbitals that contribute to the SHG effect in the real space, the SHG-weighted charge density analysis tool and band-resolved analysis[15] were employed. Moreover, in order to analyze the contribution of an ion (or ionic group) to the SHG effect, a real-space atom-cutting technique was adopted.[16]

Table S1. Crystal data and structure refinement for $Ba_4Ca(B_2O_5)_2F_2$

Empirical formula	$Ba_4Ca(B_2O_5)_2F_2$
Formula weight	830.68
Temperature	299(2) K
Wavelength	0.71073 Å
Crystal system	Monoclinic
space group	$P2_1$
Unit cell dimensions	a = 8.3888(5) Å
	b = 8.8692(6) Å
	c = 8.5608(6) Å
	β = 106.684(2)°
Volume	610.13(7) Å^3
Z	2
Density (g/cm^3)	4.522
Absorption coefficient (mm^{-1})	13.225
F(000)	724
Crystal size	0.056 mm × 0.058 mm × 0.074 mm
Theta range for data collection	2.48 to 27.51°
Limiting indices	$-10 \leq h \leq 10$, $-11 \leq k \leq 11$, $-11 \leq l \leq 11$
Reflections collected / unique	5780 / 2787 [R(int) = 0.0260]
Completeness to θ = 25.242°	100.0 %
Data/restraints/parameters	2787 / 1 / 190
Goodness-of-fit on F^2	1.042
Final R indices [$F_o{}^2 > 2\sigma(F_o{}^2)$][a]	R_1 = 0.0276, wR_2 = 0.0619
R indices (all data)[a]	R_1 = 0.0296, wR_2 = 0.0635
Flack parameter	0.02(3)
Largest peak and hole	1.70/-1.18 eÅ^{-3}

[a] $R_1 = \Sigma||F_o| - |F_c||/\Sigma|F_o|$ and $wR_2 = [\Sigma w(F_o{}^2 - F_c{}^2)^2 / \Sigma w\, F_o{}^4]^{1/2}$ for $F_o{}^2 > 2\sigma(F_o{}^2)$

Table S2. Atomic coordinates (x 10^4) and equivalent isotropic displacement parameters (A^2 x 10^3) for $Ba_4Ca(B_2O_5)_2F_2$. U(eq) is defined as one third of the trace of the orthogonalized Uij tensor.

Atoms	x	y	z	U(eq)	BVS
Ba(1)	1857(1)	5745(1)	3316(1)	18(1)	1.67
Ba(2)	2160(1)	4054(1)	8666(1)	16(1)	1.93
Ba(3)	2584(1)	-527(1)	9914(1)	17(1)	1.87
Ba(4)	2519(1)	10525(1)	4884(1)	14(1)	1.97
Ca(1)	5108(3)	7516(3)	7499(3)	14(1)	2.45
B(1)	4812(18)	3585(18)	6355(19)	18(3)	3.10
B(2)	1111(15)	7210(17)	6679(17)	16(3)	3.02
B(3)	4775(17)	6404(18)	1409(16)	13(3)	3.10
B(4)	-470(16)	6996(16)	8784(16)	16(3)	2.88
O(1)	5752(16)	8462(15)	5261(14)	51(3)	1.95
O(2)	635(11)	6161(13)	9894(12)	36(3)	1.78
O(3)	7893(10)	7187(11)	8701(11)	22(2)	1.96
O(4)	782(10)	5803(10)	6064(10)	21(2)	2.03
O(5)	4530(13)	4963(14)	1601(18)	48(4)	2.03
O(6)	2348(11)	8102(11)	6508(13)	30(2)	2.04
O(7)	4921(13)	7156(15)	102(14)	40(3)	1.92
O(8)	61(14)	7819(11)	7544(14)	36(3)	2.02
O(9)	4790(14)	7166(13)	2893(14)	40(3)	2.13
O(10)	4964(15)	4919(15)	7120(20)	72(5)	1.92
F(1)	1471(9)	1344(9)	7391(9)	21(2)	1.09
F(2)	1377(10)	8621(10)	2429(10)	30(2)	0.95

Table S3. Bond lengths (Å) and angles (deg) for $Ba_4Ca(B_2O_5)_2F_2$

Ba1–F2	2.659(9)	Ba4–F1#10	2.644(7)
Ba1–F1#1	2.733(7)	Ba4–F2	2.651(8)
Ba1–O4	2.751(8)	Ba4–O4#1	2.664(8)
Ba1–O2#2	2.837(10)	Ba4–O9#11	2.893(12)
Ba1–O1#3	2.864(13)	Ba4–O1#11	3.002(13)
Ba1–O9	2.879(10)	Ba4–O10#11	3.124(17)
Ba1–O8#4	3.031(10)	Ba4–O1	3.210(13)
Ba1–O5	3.091(12)	Ba4–O8#1	3.250(11)
Ba2–F1	2.635(8)	Ca1–O6	2.285(9)
Ba2–O2	2.647(9)	Ca1–O3	2.285(8)
Ba2–O4	2.688(9)	Ca1–O5#11	2.294(12)
Ba2–O3#5	2.808(9)	Ca1–O1	2.294(11)
Ba2–O5#6	2.837(14)	Ca1–O7#6	2.301(11)
Ba2–F2#4	2.869(8)	Ca1–O10	2.325(13)
Ba2–O7#3	2.908(12)	B1–O1#3	1.332(19)
Ba2–O10	3.110(16)	B1–O10	1.34(2)
Ba3–F1	2.670(8)	B1–O9#3	1.409(19)
Ba3–F2#7	2.736(8)	B2–O6	1.346(16)
Ba3–O3#5	2.763(9)	B2–O4	1.352(18)
Ba3–O10#5	2.801(15)	B2–O8	1.410(17)
Ba3–O7#7	2.812(12)	B3–O5	1.312(17)
Ba3–O8#8	2.878(12)	B3–O7	1.338(17)
Ba3–O5#3	3.088(12)	B3–O9	1.436(18)
Ba3–O6#8	3.113(11)	B4–O2	1.343(16)
Ba3–O2#9	3.134(11)	B4–O3#12	1.364(15)
Ba3–O7#3	3.172(12)	B4–O8	1.460(16)
Ba4–O6	2.585(9)	O4–Ba1–O2#2	140.4(2)
O4–Ba1–O1#3	90.6(3)	O2–Ba2–O4	77.3(3)
O2#2–Ba1–O1#3	122.2(3)	O2–Ba2–O3#5	88.7(3)
O4–Ba1–O9	127.0(3)	O4–Ba2–O3#5	154.6(2)
O2#2–Ba1–O9	83.2(3)	O2–Ba2–O5#6	75.1(3)
O1#3–Ba1–O9	81.0(4)	O4–Ba2–O5#6	126.5(3)
O4–Ba1–O8#4	86.7(3)	O3#5–Ba2–O5#6	68.0(3)
O2#2–Ba1–O8#4	81.5(3)	O2–Ba2–O7#3	135.8(3)
O1#3–Ba1–O8#4	75.9(3)	O4–Ba2–O7#3	138.7(3)
O9–Ba1–O8#4	139.3(3)	O3#5–Ba2–O7#3	64.7(3)
O4–Ba1–O5	150.6(3)	O5#6–Ba2–O7#3	62.6(3)
O2#2–Ba1–O5	68.6(3)	O2–Ba2–O10	120.4(4)
O1#3–Ba1–O5	61.9(3)	O4–Ba2–O10	72.7(3)
O9–Ba1–O5	43.6(3)	O3#5–Ba2–O10	132.5(3)
O8#4–Ba1–O5	95.7(3)	O5#6–Ba2–O10	83.3(4)
O3#5–Ba3–O7#7	142.8(3)	O7#3–Ba2–O10	68.7(3)
O3#5–Ba3–O10#5	69.3(4)	O6–Ba4–O4#1	91.6(3)

O10#5–Ba3–O7#7	74.5(4)	O4#1–Ba4–O1	149.1(3)
O3#5–Ba3–O8#8	125.4(3)	O9#11–Ba4–O1	75.1(3)
O10#5–Ba3–O8#8	155.7(3)	O1#11–Ba4–O1	95.41(11)
O7#7–Ba3–O8#8	91.6(3)	O10#11–Ba4–O1	43.3(3)
O3#5–Ba3–O5#3	106.6(3)	O6–Ba4–O8#1	137.3(3)
O10#5–Ba3–O5#3	84.3(4)	O4#1–Ba4–O8#1	45.9(3)
O7#7–Ba3–O5#3	60.6(3)	O9#11–Ba4–O8#1	110.9(3)
O8#8–Ba3–O5#3	106.4(3)	O1#11–Ba4–O8#1	70.8(3)
O3#5–Ba3–O6#8	139.9(3)	O10#11–Ba4–O8#1	100.8(3)
O10#5–Ba3–O6#8	137.6(4)	O1–Ba4–O8#1	144.0(3)
O7#7–Ba3–O6#8	67.9(3)	O6–Ca1–O3	172.8(4)
O8#8–Ba3–O6#8	45.9(2)	O6–Ca1–O5#11	86.1(4)
O5#3–Ba3–O6#8	60.5(3)	O3–Ca1–O5#11	87.1(4)
O3#5–Ba3–O2#9	47.8(2)	O6–Ca1–O1	93.6(4)
O10#5–Ba3–O2#9	107.7(4)	O3–Ca1–O1	88.1(4)
O7#7–Ba3–O2#9	160.6(3)	O5#11–Ca1–O1	83.9(5)
O8#8–Ba3–O2#9	79.1(3)	O6–Ca1–O7#6	92.7(4)
O5#3–Ba3–O2#9	138.3(3)	O3–Ca1–O7#6	83.8(4)
O6#8–Ba3–O2#9	114.3(2)	O5#11–Ca1–O7#6	81.1(5)
O3#5–Ba3–O7#3	61.7(2)	O1–Ca1–O7#6	163.3(5)
O10#5–Ba3–O7#3	65.5(4)	O6–Ca1–O10	99.6(4)
O7#7–Ba3–O7#3	95.66(3)	O3–Ca1–O10	86.7(4)
O8#8–Ba3–O7#3	137.1(3)	O5#11–Ca1–O10	168.9(6)
O5#3–Ba3–O7#3	45.1(3)	O1–Ca1–O10	105.1(6)
O6#8–Ba3–O7#3	98.8(3)	O7#6–Ca1–O10	89.0(6)
O2#9–Ba3–O7#3	102.8(3)	O1#3–B1–O10	122.3(15)
O6–Ba4–O9#11	102.6(3)	O1#3–B1–O9#3	111.6(13)
O4#1–Ba4–O9#11	134.4(3)	O10–B1–O9#3	126.1(14)
O6–Ba4–O1#11	147.7(3)	O6–B2–O4	125.3(12)
O4#1–Ba4–O1#11	112.3(3)	O6–B2–O8	116.7(12)
O9#11–Ba4–O1#11	45.2(3)	O4–B2–O8	118.0(11)
O6–Ba4–O10#11	107.6(3)	O5–B3–O7	130.2(15)
O4#1–Ba4–O10#11	131.0(3)	O5–B3–O9	108.0(13)
O9#11–Ba4–O10#11	85.7(3)	O7–B3–O9	121.7(14)
O1#11–Ba4–O10#11	73.5(3)	O2–B4–O3#12	125.8(12)
O6–Ba4–O1	69.4(3)	O2–B4–O8	119.8(11)
O3#12–B4–O8	114.4(11)		

Symmetry transformations used to generate equivalent atoms:

#1: -X, 0.5+Y, 1-Z;   #2: +X, +Y, -1+Z;   #3: 1-X, -0.5+Y, 1-Z;   #4: -X, -0.5+Y, 1-Z;   #5: 1-X, -0.5+Y, 2-Z;   #6: +X, +Y, 1+Z;   #7: +X, -1+Y, 1+Z;   #8: +X, -1+Y, +Z;   #9: -X, -0.5+Y, 2-Z;   #10: +X, 1+Y, +Z;   #11: 1-X, 0.5+Y, 1-Z;   #12: -1+X, +Y, +Z;   #13: 1-X, 0.5+Y, 2-Z;   #14: +X, 1+Y, -1+Z;   #15: -X, 0.5+Y, 2-Z;   #16: 1+X, +Y, +Z;

Table S4. Summary of NLO crystals with B_2O_5 groups concerning on the two critical properties, SHG effect and absorption edge. $Ba_4Ca(B_2O_5)_2F_2$ exhibits the largest SHG effect in the DUV compounds with B_2O_5 groups.

X cations include transition metals or second-order Jahn-Teller effect (SOJT) cations.

Table S4a. Summary of NLO crystals with only B_2O_5 groups.

Compounds	Space group	X cations	B-O groups	SHG effect (×KDP)	Cut-off edge (nm) Or Band gap
$Ba_4Ca(B_2O_5)_2F_2$	$P2_1$	/	B_2O_5	2.2	<190
α-$Li_4B_2O_5$[17]	$Pca2_1$	/	B_2O_5	0.3	178
$Li_6CuB_4O_{10}$[18]	$P1$	Cu^{2+}	B_2O_5	1.0	610
$BaCuB_2O_5$[19]	$C2$	Cu^2	B_2O_5	N/A	N/A
$KSbB_2O_6$[20]	Cc	Sb^{5+}	B_2O_5	weak	3.63eV
$KSbOB_2O_5$[21]	$Pmn2_1$	Sb^{5+}	B_2O_5	N/A	N/A
$RbSbB_2O_6$[22]	Cc	Sb^{5+}	B_2O_5	weak	3.64 eV
$RbSbB_2O_6$[23]	$Pmn2_1$	Sb^{5+}	B_2O_5	[b]0.9	N/A
$KNbB_2O_6$[24]	$Pna2_1$	Nb^{5+}	B_2O_5	7.0	265
$CsNbOB_2O_5$[24]	$Pmn2_1$	Nb^{5+}	B_2O_5	5.0	277
$RbNbB_2O_6$[24]	$Pna2_1$	Nb^{5+}	B_2O_5	5.0	270
$KTaOB_2O_5$[23]	$Pmn2_1$	Ta^{5+}	B_2O_5	[b]0.9	N/A
$RbTaOB_2O_5$[23]	$Pmn2_1$	Ta^{5+}	B_2O_5	[b]1.0	N/A
$CsTaOB_2O_5$[23]	$Pmn2_1$	Ta^{5+}	B_2O_5	[b]1.0	N/A
$RbTlB_2O_6$[24]	/	Tl^+	B_2O_5	N/A	N/A
$TlNbB_2O_6$[25]	$Pna2_1$	Tl^+,Nb^{5+}	B_2O_5	N/A	N/A
$TlTaB_2O_6$[25]	$Pmn2_1$	Tl^+,Ta^{5+}	B_2O_5	N/A	N/A

b: $44\times SiO_2=1\times KDP$

Table S4b. Summary of NLO crystals with B_2O_5 groups and other B-O groups.

Compounds	Space group	X cations	B-O groups	SHG effect (×KDP)	Cut-off edge (nm) Or Band gap
$NaBe_4B_4O_{11}$[26]	$P1$	/	$^cB_2O_5+BO_3$	1.3	171
$Na_5LiBe_{12}B_{12}O_{33}$[26]	Pc	/	$^cB_2O_5+BO_3$	1.4	169
$Ba_5(BO_3)_2(B_2O_5)$[27]	$P2_12_12_1$	/	$B_2O_5+BO_3$	N/A	N/A
α-$Pb_2Ba_4Zn_4B_{14}O_{31}$[28]	$P1$	Pb^{2+}	$^cB_2O_5+B_6O_{13}$	0.6	289
β-$Pb_2Ba_4Zn_4B_{14}O_{31}$[28]	Cc	Pb^{2+}	$^cB_2O_5+B_6O_{13}$	1.1	303
γ-$Pb_2Ba_4Zn_4B_{14}O_{31}$[28]	$P3_2$	Pb^{2+}	$^cB_2O_5+B_6O_{13}$	N/A	3.47 eV
$Pb_3Ba_7B_7O_{20}F$[29]	$Pmn2_1$	Pb^{2+}	$B_2O_5+BO_3$	5.0	286
$Pb_4O(BO_3)_2$[30]	$Aba2$	Pb^{2+}	$^cB_2O_5+BO_3$	3.0	280
$Bi_2ZnOB_2O_6$[31]	$Pba2$	Bi^{3+}	$B_2O_5+B_2O_7$	3~4	330

c: means that B_2O_5 dimers serve as a connection in the structure and contribute little to the total SHG effects.

N/A means not given in the related reference.

Table S5a. The calculated SHG coefficients of $Ba_4Ca(B_2O_5)_2F_2$ and $\alpha\text{-Li}_4B_2O_5$.

Compounds	Eg (eV)		d_{ij} (pm/V)
	PBE	PBE0	
$Ba_4Ca(B_2O_5)_2F_2$ ($P2_1$)	3.985	6.343	d_{16}=0.197 d_{14}=-0.298 d_{22}=-0.524 d_{23}=0.423
$\alpha\text{-Li}_4B_2O_5$ ($Pca2_1$)	4.36	6.966 (experimental)	d_{15}=-0.016 d_{24}=-0.102 d_{33}=0.034

Table S5b. The real-space atom-cutting of $Ba_4Ca(B_2O_5)_2F_2$.

	d_{16}	d_{14}	d_{22}	d_{23}
Ba	0.074	-0.083	-0.062	0.146
Ca	0.009	-0.018	-0.005	0.020
B_2O_5	0.047	-0.104	-0.240	0.082
F	-0.0007	-0.010	-0.023	0.002
$Ba_4Ca(B_2O_5)_2F_2$	0.197	0.298	-0.524	0.423
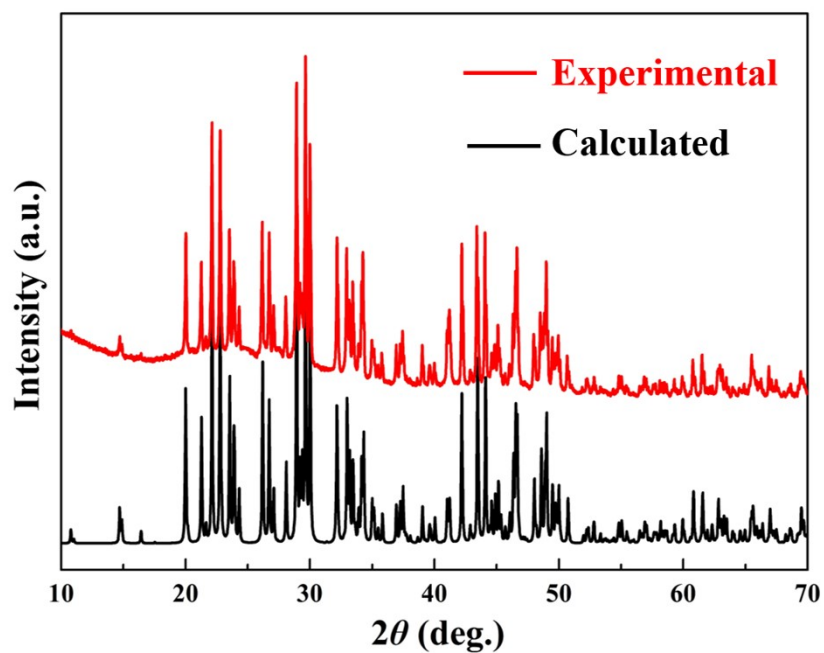
Figure S1. The experimental and calculated sample XRD patterns of $Ba_4Ca(B_2O_5)_2F_2$.
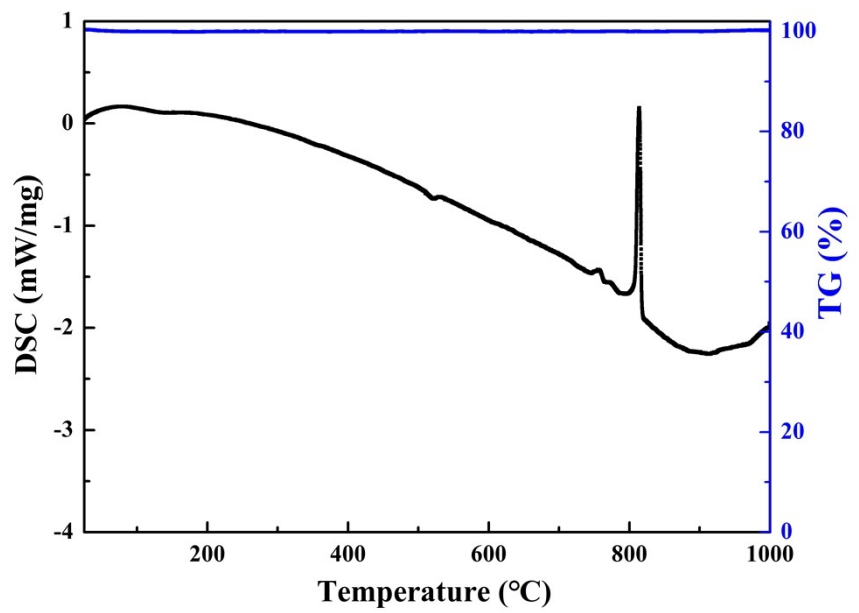
Figure S2. The TG-DSC curves of $Ba_4Ca(B_2O_5)_2F_2$.
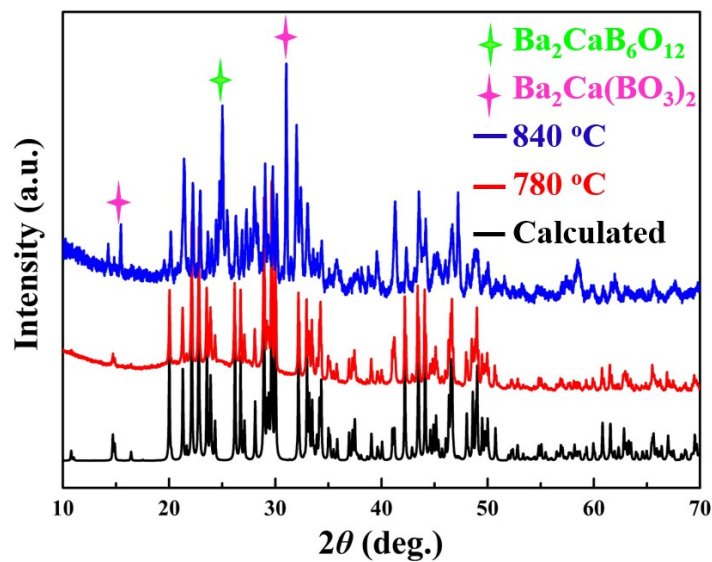
Figure S3. The experimental XRD patternts at different temperatures and calculated XRD pattern of
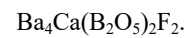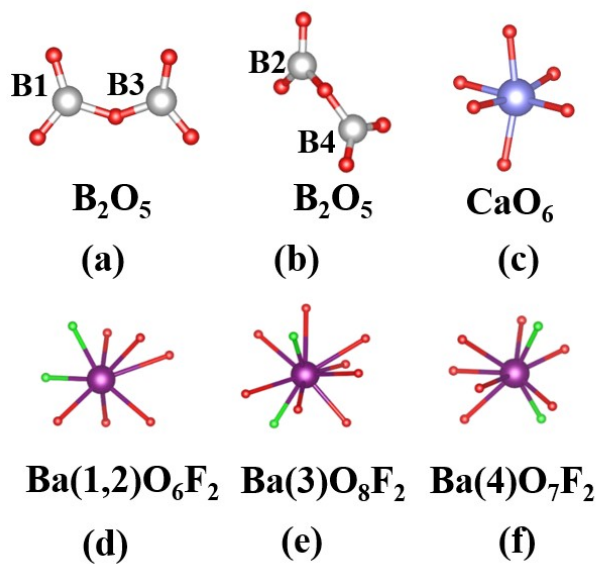
Ba$_4$Ca(B$_2$O$_5$)$_2$F$_2$.

Figure S4. (a) Plane B $(1,3)_2O_5$ units, (b) distorted B $(2,4)_2O_5$. (c) CaO_6 octahedra, (d-f) Three different types of coordination environments of Ba^{2+} cations in $Ba_4Ca(B_2O_5)_2F_2$.
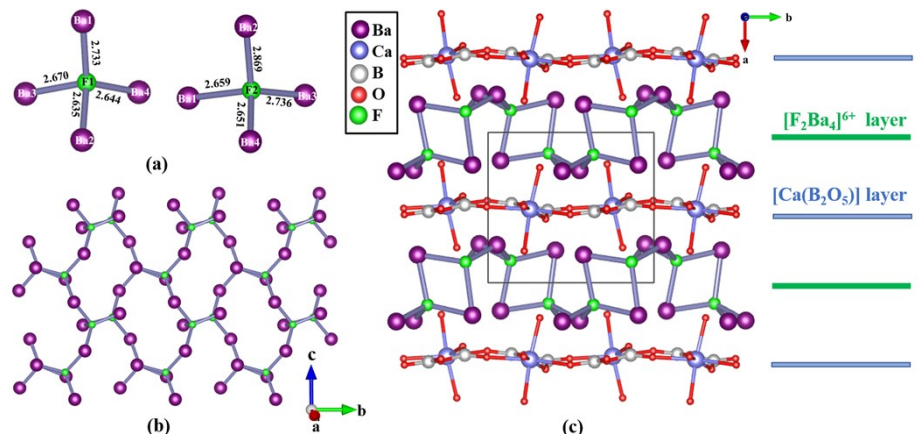
Figure S5. (a) Distorted FBa$_4$ tetrahedra, (b) 2D [F$_2$Ba$_4$] infinite layer and (c) [F$_2$Ba$_4$] layers and [Ca(B$_2$O$_5$)] layers alternately stack along the a-axis.
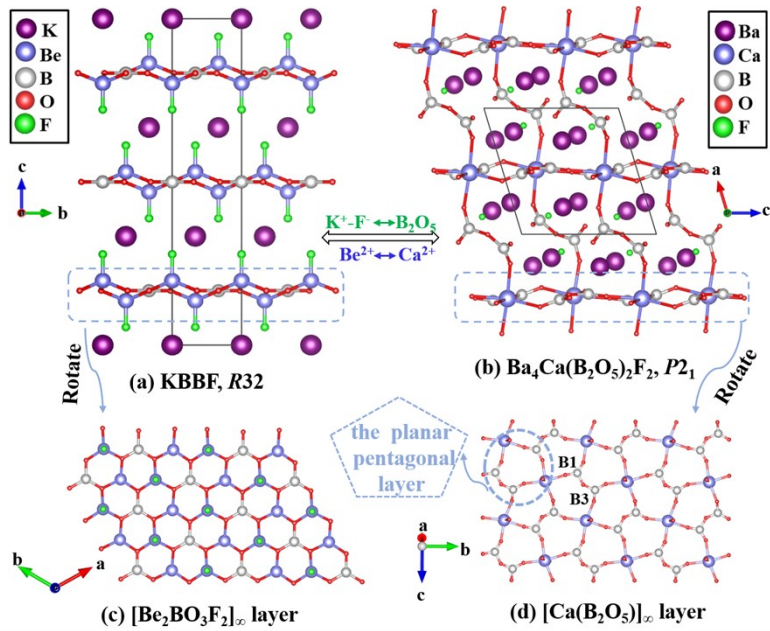
Figure S6. The structural evolution from KBBF to $Ba_4Ca(B_2O_5)_2F_2$. (a) Crystal structure of KBBF. (b) Crystal structure of $Ba_4Ca(B_2O_5)_2F_2$. (c) The $[Ca(B_2O_5)]_\infty$ layered structure. (d) The $[Ca(B_2O_5)]_\infty$ layer is composed of B_2O_5 and CaO_6.
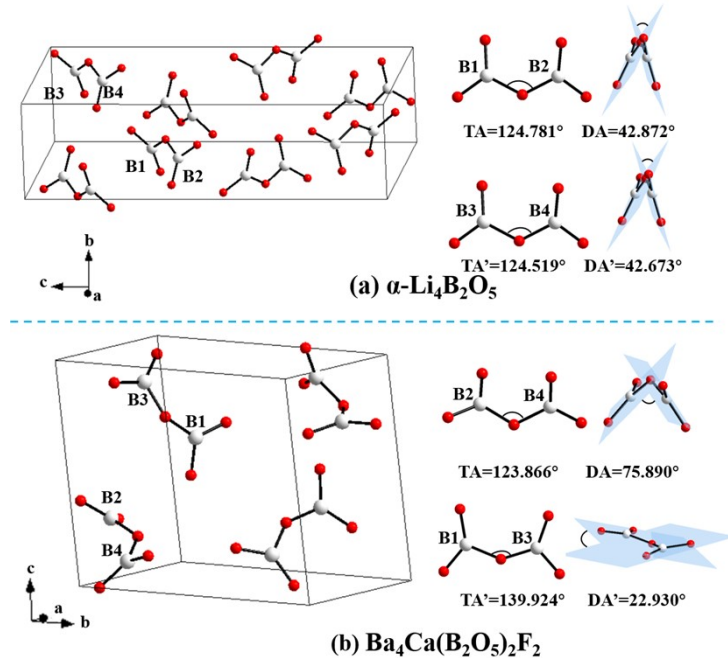
Figure S7. The arrangements of B_2O_5 units in (a) α-$Li_4B_2O_5$ and (b) $Ba_4Ca(B_2O_5)_2F_2$, where DA is the dihedral angle (angle between two BO_3 planes). TA is the torsion angle (B−O−B angle between two connected BO_3 units).

As shown in Figure S7, the values of TAs are similar in both compounds, while the DAs have obvious differences. We can see that two kinds of twisted B_2O_5 groups in α-$Li_4B_2O_5$ have large DAs, 42.872° and 42.873°. While in $Ba_4Ca(B_2O_5)_2F_2$, the DAs of B_2O_5 (B(2)B(4)O_5) groups have a similar feature with twisted B_2O_5 groups in α-$Li_4B_2O_5$, and the DAs of the B_2O_5 (B(2)B(4)O_5) are 75.890. Differently, in $Ba_4Ca(B_2O_5)_2F_2$, the DAs of the B_2O_5 (B(1)B(3)O_5) in the planar pentagonal tiling [Ca(B_2O_5)] layers are 22.930°, indicating that two constitute BO_3 triangles adopt nearly coplanar arrangements, which is benefit to a large SHG response.
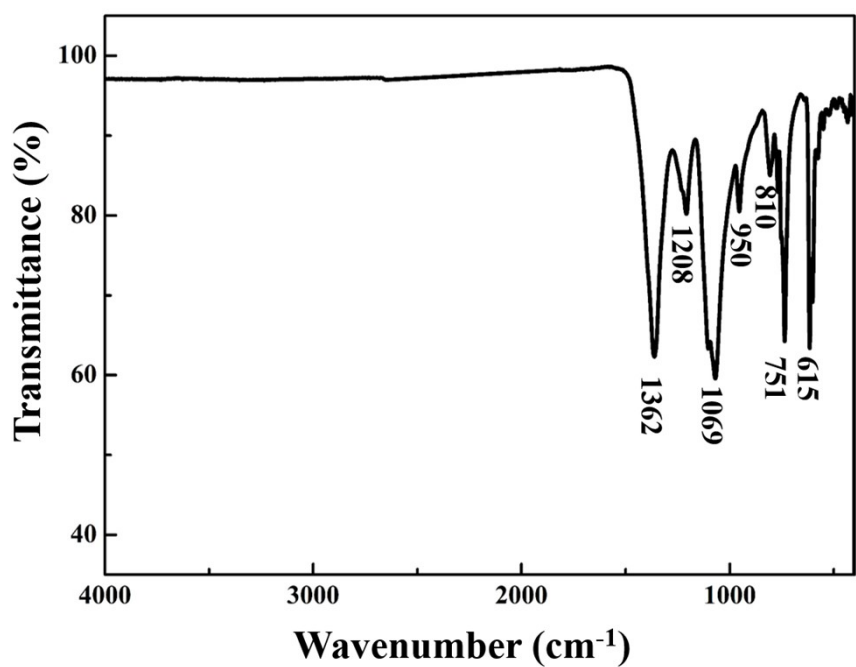
Figure S8. The IR spectrum of $Ba_4Ca(B_2O_5)_2F_2$.
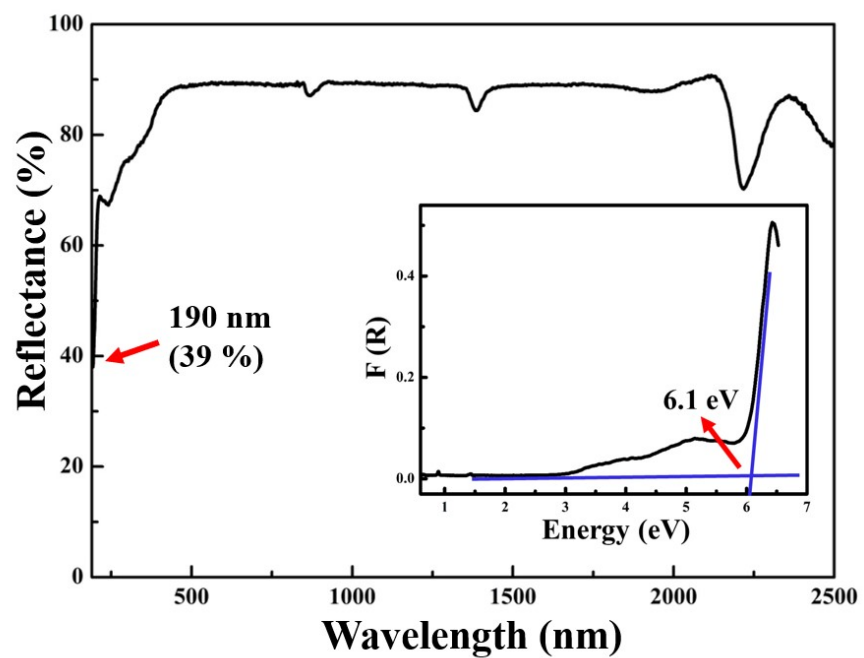
Figure S9. The UV-vis-NIR diffuse reflectance spectrum of $Ba_4Ca(B_2O_5)_2F_2$.
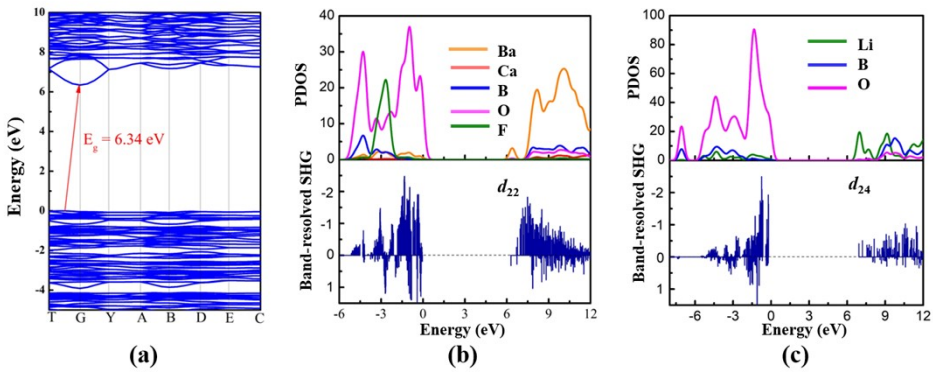
Figure S10. (a) Calculated band structure of $Ba_4Ca(B_2O_5)_2F_2$. The band-resolved SHG of (b) $Ba_4Ca(B_2O_5)_2F_2$ and (c) α-$Li_4B_2O_5$.

References

1. G. M. Sheldrick, *Acta Crystallogr. Sect. A: Found. Adv*., 2015, **71**, 3-8.

2. G. M. Sheldrick, *Acta Crystallogr. Sect. A*., 2008, **64**, 112-122.

3. A. L. Spek, *J. Appl. Crystallogr*., 2003, **36**, 7-13.

4. P. Kubelka, and F. Z. Munk, *Tech. Phys.,* 1931, **12**, 593-601.

5. J. Tauc, *Mater. Res. Bull.,* 1970, **5**, 721-730.

6. S. K. Kurtz and T. T. Perry, *J. Appl. Phys*., 1968, **39**, 3798-3813.

7. M. C. Payne, M. P. Teter, D. C. Allan, T. A. Arias and J. D. Joannopoulos, *Rev. Mod. Phys*., 1992, **64**, 1045-1097.

8. S. J. Clark, M. D. Segall, C. J. Pickard, P. J. Hasnip, M. J. Probert, K. Refson and M. C. Payne, Z. *Kristallogr*., 2005, **220**, 567-570.

9. W. Kohn, *Rev. Mod. Phys.*, 1999, **71**, 1253–1266.

10. M. G. Medvedev, I. S. Bushmarinov, J. Sun, J. P. Perdew and K. A. Lyssenko, *Science.*, 2017, **355**, 49–52.

11. H. J. Monkhorst and J. D. Pack, *Phys. Rev. B*., 1976, **13**, 5188-5192.

12. D. M. Ceperley and B. J. Alder, *Phys. Rev. Lett*., 1980, **45**, 566-569.

13. S. N. Rashkeev, W. R. Lambrecht and B. Segall, *Phys. Rev*. B., 1998, **57**, 3905-3919.

14. J. Lin, M. H. Lee, Z. P. Liu, C. T. Chen and C. J. Pickard, *J. Phys. Rev. B*., 1999, *60*, 13380-13389.

15. M. H. Lee, C. H. Yang and J. H. Jan, *Phys. Rev. B*., 2004, **70**, 235110-235120.

16. L. Kang, F. Liang, X. X. Jiang, Z. S. Lin and C. T. Chen, *Acc. Chem. Res*. 2020, *53*, 209-217.

17. M. He, H. Okudera, A. Simon, J. Köhler, S. Jin and X. Chen, *J. Solid State Chem.*, 2013, **197**, 466–470.

18. S. Pan, J. P. Smit, B. Watkins, M. R. Marvel, C. L. Stern and K. R. Poeppelmeier, *J. Am. Chem. Soc.*, 2006, **128**, 11631–11634.

19 Z He and W Cheng, *J. Solid State Chem.,* 2009, **149**,236-238.

20 C. Huang, J. H. Zhang, C. L. Hu, X. Xu, F. Kong and J. G. Mao, *Inorg. Chem.*, 2014, **53**, 3847–3853.

21 D. Zhao, R. H. Zhang, F. F. Li, J. Yang, B. G. Liu and Y. C. Fan, *Dalt. Trans.*, 2015, **44**, 6277–6287.

22 D. Yan, C. L. Hu and J. G. Mao, *CrystEngComm.*, 2016, **18**, 1655–1664.

23 J. Gopalakrishnan, K. Ramesha, K. Kasthuri Rangan and S. Pandey, *J. Solid State Chem.*, 1999, **148**, 75–80.

24 J. F. H. Nicholls, B. Henderson and B. H. T. Chai, *Opt. Mater.,* 2001, **16**, 453-462.

25 S. Schmid and T. Wagner, *Acta Crystallogr. Sect. B Struct. Sci.*, 2005, **61**, 361–366.

26 H. Huang, L. Liu, S. Jin, W. Yao, Y. Zhang and C. Chen, *J. Am. Chem. Soc.*, 2013, **135**, 18319–18322.

27 N. G. Furmanova, B. A. Maksimov, V. N. Molchanov, A. E. Kokh, N. G. Kononova en P. P. Fedorov, *Crystallogr. Reports*, 2006, **51**, 219–224.

28 H. Yu, H. Wu, Q. Jing, Z. Yang, P. S. Halasyamani and S. Pan, *Chem. Mater.*, 2015, **27**, 4779–4788.

29 W. Zhang, W. Jin, S. Han, Z. Yang and S. Pan, *Scr. Mater.*, 2021, **194**, 113700.

30 H. Yu, S. Pan, H. Wu, W. Zhao, F. Zhang, H. Li and Z. Yang, *J. Mater. Chem.*, 2012, **22**, 2105–2110.

31 F. Li, X. Hou, S. Pan and X. Wang, *Chem. Mater.*, 2009, **21**, 2846–2850.